CWE-8
June 7-11, 2026
London. ON. Canada

Towards Reliable CFD Validation from Wind Tunnel Studies of the Flow in a Street Canyon

Maria Kotsiopoulou [a1], Nikolaos Petros Pallas [a2], Demetri Bouris [a3]

[a]*School of Mechanical Engineering, National Technical University of Athens, Greece*
[1]mkotsiopoulou@mail.ntua.gr,[2]npallas@mail.ntua.gr,[3]dbouris@fluid.mech.ntua.gr

SUMMARY

The flow in street canyons has been extensively studied in wind tunnels under varying geometric and inflow conditions. However, discrepancies persist, even for nominally identical configurations following established guidelines, introducing uncertainties for CFD validation. This study is motivated by the radically different flows measured in two wind tunnels for geometrically identical canyon arrays. CFD simulations of the full experimental setup reproduce the flow structure of one experiment, where no in-canyon vortex is formed while single canyon setups, using measured upstream profiles or periodic inflow-outflow conditions, reproduce the in-canyon vortex measured in the other experiment and agree with the literature. For the single canyon, both steady RANS and unsteady LES reproduce a similar in-canyon vortex, with variations in its position depending on its spanwise extents. Further simulations show that upstream flow conditions strongly influence the in-canyon flow. Validation studies lacking detailed inflow information may therefore be significantly affected by non-model-related uncertainties.

Keywords: *Street Canyon, Computational Fluid Dynamics, Validation, Large Eddy Simulation, Wind Tunnel*

1. INTRODUCTION

Urban street canyons are a fundamental flow unit for studying wind and pollutant transport in cities. Canyons with height to width ratio (H/W) of 1 are a simple yet representative benchmark geometry for both wind tunnel experiments and Computational Fluid Dynamics (CFD) studies, due to their relative simplicity and relevance to real urban environments. Within this framework, the recent TWEET-IE project (TWEET-IE,2021; Pallas et al., 2025; Dsouza et al., 2025) carried out a twin experimental campaign in two different wind tunnel facilities: a closed-loop wind tunnel at NTUA and an open-jet facility at TU Delft. In both experiments, an identical multi-canyon configuration was employed, consisting of a splitter plate on which a six consecutive building array (height/width, H/W=1, length/width, L/W=8) was mounted, aligned perpendicular to the approaching flow. The splitter plate was elevated above the height of the boundary layer in the NTUA wind tunnel, to ensure a uniform approach flow for both experiments. Free stream turbulence levels in both facilities were below 1%. Dimensions of the building array were chosen according to literature guidelines to eliminate spanwise canyon flow and ensure similar in-canyon behaviour downstream of the 3rd-4th canyon (Hunter et al., 1990 and Chew and Norford, 2018). Measurements focused on the fourth canyon using Particle Tracking Velocimetry (PTV) in both facilities and employing the same seeding material. The blockage ratio was below 5% in the NTUA wind tunnel and much lower at TU Delft. Despite the nominally identical geometry, efforts to ensure similar upstream flow and application of the same measurement technique, the measured flow fields differed significantly, even at the level of their basic topology. In particular, at the canyon mid-plane a well defined recirculation vortex was observed in the NTUA experiments, but not in the TU Delft measurements. The mid-plane streamwise velocity contours and velocity vectors for both measurement sets are presented in Figure 1.

Motivated by this inconsistency between the two nominally identical experiments, a detailed review of the conditions and setups in the literature was performed. Several wind tunnel studies have examined the flow in street canyons with H/W=1 under varying inflow and geometric conditions. Kovar-Panskus et al. (2002) investigated a long isolated canyon (L/H=12.9) exposed to turbulence generated by a grid, vortex generators and fences while Allegrini et al. (2013) also studied an isolated canyon (L/H=9) in a closed-loop tunnel but with a thin upstream boundary layer approaching over an effectively infinitely long upstream building roof (i.e. a submerged canyon). In both cases, the canyon span was comparable to the width of the wind tunnel, effectively eliminating lateral inflow. Uehara et al. (2000) used an array of cubic blocks with a rough upstream atmospheric boundary layer (ABL) whereas Lin et al. (2021) embedded the target canyon within a 25-row array of buildings (L/W=10). Despite the differences, all of these studies reported a single, centrally located recirculation cell within the canyon. One of the few literature studies that was found to differ from this flow structure was that of Cui et al. (2014), who studied a short canyon of L/W=3, exposed to a rough upstream ABL, and found the recirculation cell shifted away from the canyon centre. 3D effects may be a factor, due to the short spanwise length (L/W<7, Hunter et al., 1990).

Figure 2 shows that, despite differing experimental configurations, most datasets yield similar velocity profiles at the centerline of the canyon, except for the short canyon (L/W=3), where the flow also exhibits much higher shear at roof level. Indeed, in a recent LES study, Zhu and Chew (2025) observed that the above-canyon boundary layer shear plays a key role in determining the in-canyon vortex structure and also showed that significant spanwise motion persists even for canyons with L/W=10. Consistently, previous CFD studies have also shown that the canyon flow is governed by the interaction between the shear layer forming at roof level due to flow separation and three-dimensional effects such as lateral entrainment in finite-length canyons (Li et al., 2021). Together, these mechanisms indicate that the in-canyon vortex structure may be sensitive to both the above-canyon flow and the canyon aspect ratio (L/W). However, in the case of the two TWEET-IE experiments, the spanwise length is the same, suggesting that the discrepancies may be attributed to differences in the above canyon flow, directly linked to the approaching flow. Intriguingly, although the NTUA measurements show a recirculation vortex consistent with long canyon studies, the vortex is displaced away from the canyon center toward the ground and the downstream building (Figure 2). On the other hand, TU Delft measurements more closely resemble those of the short (L/W=3) canyon (Cui et al., 2014), in spite of the fact that the above canyon flow in these two datasets constitutes the upper and lower limit of above canyon shear.

In an attempt to address the effect of the parameters that differ among the two tests, a series of Reynolds Averaged Navier Stokes (RANS) and Large Eddy Simulations (LES) is performed. The initial RANS simulation takes into account the whole experimental configuration, including the elevated splitter plate, thus simulating a uniform approach flow around the full model. This effectively represents both configurations but the CFD domain is limited to the smaller of the two wind tunnels (NTUA) (Figure 1). No in-canyon vortex is observed at the mid-plane. Subsequently, a single canyon with (L/W=∞) is studied with RANS, leveraging the measured velocity profiles on the roof of the canyon's upstream building. LES simulations are also performed for a single canyon, applying periodic inflow-outflow conditions (to imply an infinite array of canyons) and for different canyon spans (L/W = ∞, 8, 4) in order to assess the influence of unsteady effects and aspect ratio on the flow. Both RANS and LES simulations for the single

canyon reproduced an in-canyon vortex at the mid-plane. Finally simulations revert to the six building array again and RANS simulations are performed. Initially with measured inflow profiles at the roof of the first building in the array and then with inflow imposed at a distance of 5H upstream of the first building in the array. Measurements were not available at this location so a set of idealized profiles is used, in order to investigate the role of upstream flow development. This investigation enables a systematic assessment of the impact of inflow definition and upstream flow evolution on the resulting canyon flow structure, and provides a consistent framework for interpreting wind tunnel data in CFD validation.

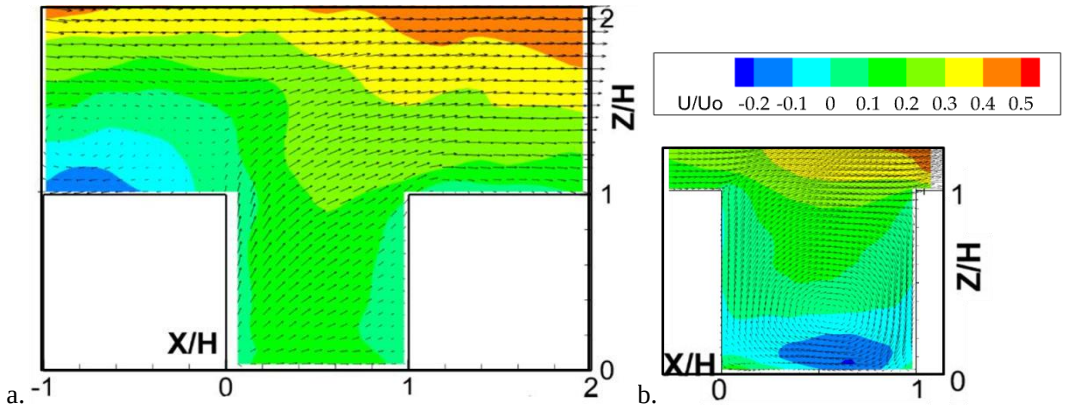

Figure 1 Streamwise velocity contours at the canyon mid-plane for (a) TU DELFT and (b) NTUA experiments.

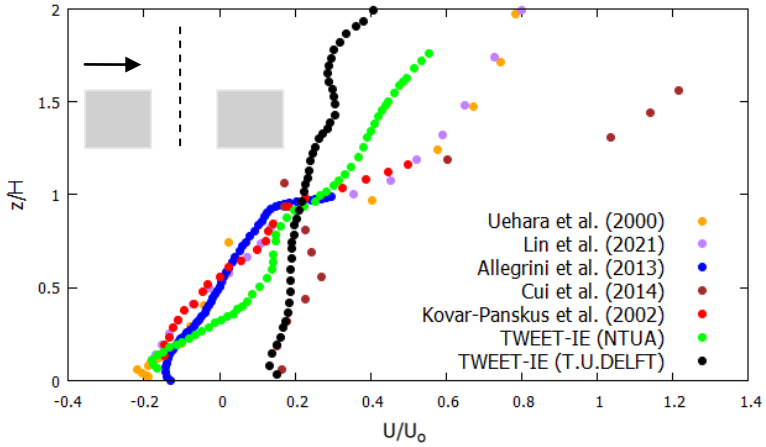

Figure 2: Comparison of Centerline Velocity Profiles from Reference Studies and TWEET-IE Measurements.

2. METHODS

2.1. Experimental campaigns in Two Wind Tunnel configurations

Measurements were primarily performed in the fourth canyon using PTV both at NTUA and TU Delft, employing Helium-filled soap bubbles as a seeding material. A more detailed description of the experiments and measurements methodologies is provided in Pallas et al. (2025) and Dsouza et al. (2025). Additionally, at NTUA, rooftop measurements of mean velocity and turbulence intensity were conducted over the first, third, fourth, and fifth buildings using both PTV and hot-wire anemometry. The approaching flow immediately upstream the splitter plate was also measured at NTUA using a Pitot tube. The experiments were conducted for several free-stream velocities (U_o), corresponding to Reynolds numbers ranging from $22\text{-}56 \cdot 10^3$ at

NTUA and from $30\text{-}100 \cdot 10^3$ at TU Delft, based on the building height (H) and a kinematic viscosity of 1.64×10^{-5} m²/s.

2.2. Numerical model

For the numerical computations, two complementary approaches and several geometric configurations were considered. Specifically, an in-house RANS solver and the open source LES framework uDALES v2.0 were employed. The in-house RANS code is a finite volume solver (Kotsiopoulou and Bouris, 2022) operating on a Cartesian collocated grid, with the SIMPLE algorithm used for pressure–velocity coupling and the RNG k–ε model for turbulence closure. The methodology employs standard wall functions, resolving the viscous and logarithmic regions in an approximate manner. In addition, uDALES v2.0 (Suter et al., 2022), an open source LES framework developed for urban atmospheric flows, was employed to investigate 3D effects. The filtered incompressible Navier–Stokes equations are solved on a Cartesian grid, with pressure obtained via FFT inversion and subgrid-scale stresses modeled using the Vreman model (Vreman, 2004). In uDALES, wall stresses are modeled using a logarithmic wall function based on aerodynamic roughness length, without explicit resolution of the viscous sublayer.

RANS simulations were first conducted for the full configuration, including the splitter plate and the building array (full-set up domain), as illustrated in Figure 3a. The inlet cross-section was defined to match the cross-sectional dimensions of the NTUA wind tunnel (3.5 m x 2.5 m), while the streamwise extent of the domain was determined following best practice guidelines (Tominaga et al., 2008), with 5H upstream and 15H downstream distances. The splitter plate was positioned at mid-span and elevated 6H above the wind tunnel floor. The inlet velocity profile in the CFD simulations was initially prescribed using a uniform velocity profile and then, again, from measurements obtained in the empty NTUA wind tunnel, prior to the installation of the experimental setup. The CFD simulations were performed for 1% free stream turbulence intensity. The computational mesh, illustrated in Figure 3b consisted of 6.75 million cells. The highest resolution was applied within the fourth canyon, where the mesh consisted of 100 x 100 cells in the streamwise (x) and vertical (z) directions. This resulted in near wall values of $y^+ < 11.6$, placing the solution within the viscous sublayer. Grid independence tests confirmed that further refinement had a negligible impact on the predicted flow.

Subsequently, simplified configurations were considered in order to isolate the role of the inflow and canyon geometry. In this context, RANS simulations were performed for an idealized single canyon corresponding to the fourth canyon, where the experimental measurements were conducted. The computational domain for the RANS simulations had dimensions of 3H x 5H in the streamwise (x) and vertical (z) directions, respectively, resulting in approximately 1 million cells. The mesh resolution within the canyon was $\Delta x = \Delta z = H/260$. The RANS setup was used to simulate an idealized infinitely long street canyon, with the computational domain corresponding to the region highlighted by the brown outline in Figure 4. The measured velocity profile at the roof level of the fourth building in the NTUA wind tunnel was prescribed at the inlet (Figure 4). To complement the RANS analysis and capture potential 3D and unsteady flow features, LES was performed and the influence of the canyon span was also examined. Three geometric configurations were investigated using uDALES: (i) an idealized infinite canyon and two finite canyons with (ii) L/W = 8 and (iii) L/W = 4. For all LES cases, the computational domain extended 4H×24H×8H in the streamwise (x), spanwise (y), and vertical (z) directions, respectively (Figure 4). The grid resolution was $\Delta x = \Delta z = H/16$ and $\Delta y = H/8$ (approximately

1.5 million cells), corresponding to $y^+ \approx 23$. The timestep satisfied $\Delta t/T < 1/1300$, where T denotes a characteristic vortex turnover time. Periodic inlet–outlet boundary conditions were applied to represent a repeating canyon sequence, with periodic lateral boundaries and a free slip condition imposed at the top of the domain. Preliminary grid sensitivity tests indicated negligible changes in the mean flow with further refinement.

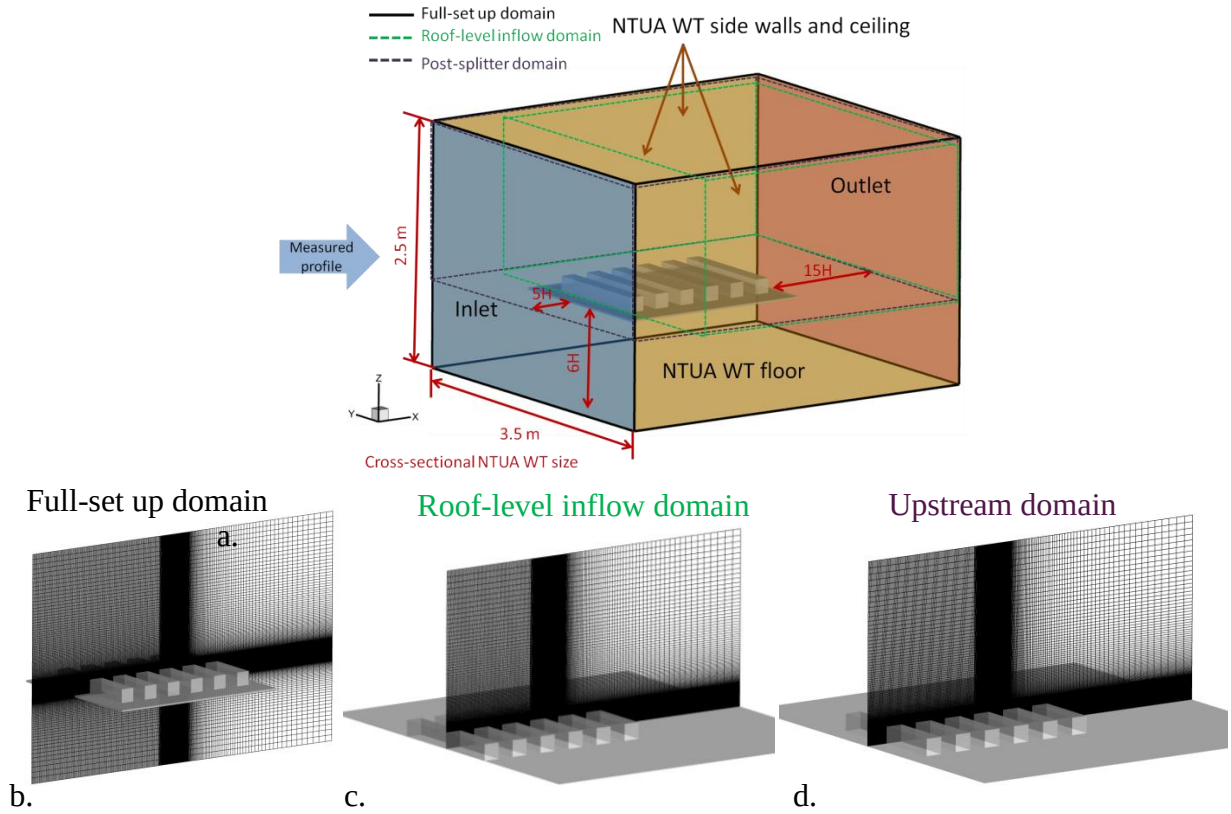

Figure 3 (a) Computational domains used in the RANS simulations, including the computational mesh of (b) the full wind tunnel configuration, (c) the roof-level inflow domain, and (d) the upstream inflow domain

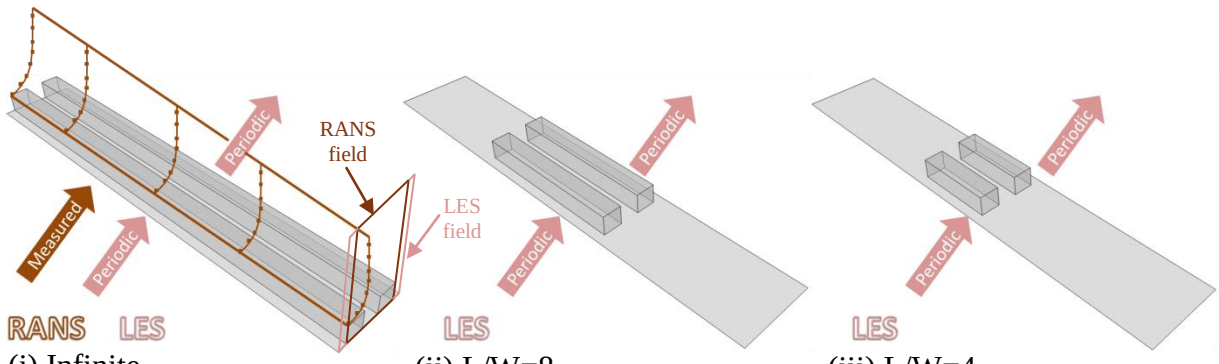

Figure 4 Schematic representation of the RANS and LES domains of the idealized single canyon configurations.

With no vortex being reproduced with simulations that include the full domain and a vortex present in RANS and LES of the single canyon, even for shorter aspect ratios, attention was directed to the upstream conditions and further RANS simulations were conducted using domains, in which the inflow was prescribed at two different streamwise locations relative to the

building array. As shown in Figure 3a, the regions enclosed by the green and purple dashed lines define two additional computational domains, namely the roof-level inflow domain and the upstream inflow domain. In the roof-level inflow domain (Figure 3c), the inflow is prescribed at the rooftop of the first building using measured velocity and turbulence profiles. In the upstream inflow domain (Figure 3d), the inflow is imposed at a distance of 5H upstream of the first building in the array. In both configurations, the splitter plate is omitted from the computational domain and focus is on the upstream flow. The grid resolution was kept consistent within the overlapping regions between the different domains. No measurements were available at 5H upstream and so the inflow conditions for this domain include both uniform velocity profiles and a set of idealized profiles characterized by a near wall logarithmic region extending up to approximately H/3 and an outer region of nearly uniform velocity. These profiles were examined for four different aerodynamic roughness lengths (z_o), in order to assess the sensitivity of the flow to near wall shear. The profiles are not intended to represent fully developed atmospheric boundary layers, but rather the flow conditions that may arise after flow interaction with the leading edge of the splitter plate, after which a new boundary layer develops while the outer flow remains relatively uniform. All simulations were performed at Reynolds numbers sufficiently high, according to ASCE (2012) and VDI (2000) standards ($>10^4$) to ensure independence of the mean flow, with $Re \approx 6 \cdot 10^4$ for RANS and $Re \approx 10^5$ for LES.

3. RESULTS

The results are first presented for the full-set up domain, which includes the elevated splitter plate (Figure 5). No significant differences were observed between the case employing a uniform inflow and that using the measured inflow from the floor of the empty wind tunnel.

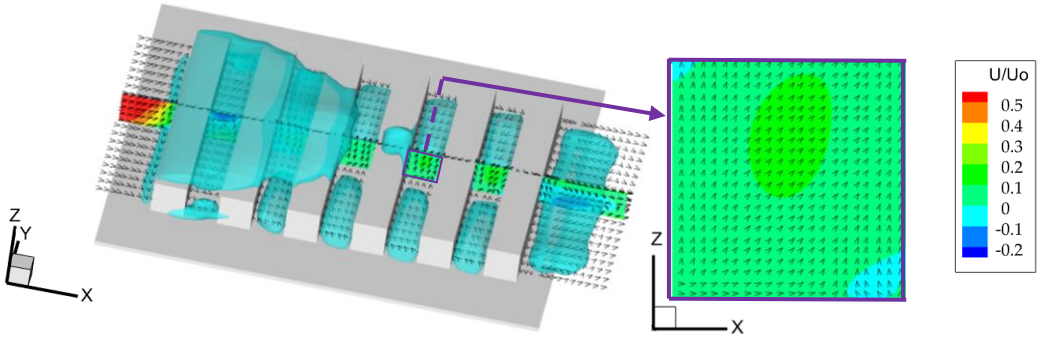

Figure 5 Velocity vectors at the vertical mid-plane and horizontal H/3 plane and streamwise velocity isosurfaces for the full-set up domain

Specifically, Figure 5 illustrates isosurfaces of the streamwise velocity, together with velocity vectors and a mid-plane distribution of the streamwise velocity. Focusing on the fourth canyon (Figure 5), it is observed that no recirculation vortex is formed within the canyon at the mid-plane and the resulting flow structure is closer to that observed in the TU Delft experiments (Figure 2). A prominent recirculation region develops above the roof of the first building and extends downstream up to approximately the third building. In addition, a secondary recirculation region is observed above the fourth building, exhibiting a structure similar to that identified in the TU Delft measurements (Figure 1a). Furthermore, the flow within the canyon doesn't exhibit a single coherent vortex in the spanwise direction, as typically observed in infinite canyons. Instead, the recirculation is disrupted as the flow approaches the canyon mid-

plane, where upward motion is observed, ejecting fluid from the canyon. This flow topology does not agree with the NTUA measurements, where the model geometry is the same but a well defined recirculation vortex exists within the canyon.

Based in this initial result, a single infinite canyon was simulated using the measured velocity profile at rooftop level as inflow. Results from this simulation show a well defined recirculation vortex within the canyon, illustrated in Figure 6a. To assess whether this behaviour is influenced by the turbulence modelling approach and/or unsteady effects, the same configuration is examined using LES (Figure 6b) employing periodic boundary conditions. The LES results show a qualitatively similar flow field, with a coherent vortex forming within the canyon, indicating that the presence of the vortex is not model dependent or attributed to the steady state approach. Therefore, attention is directed to geometric effects, and in particular to the influence of the canyon span. To this end, additional LES simulations are performed for finite-span canyons (L/W=8 and L/W=4), as shown in Figure 6c,d, respectively. Reducing the canyon span slightly alters the vortex structure for L/W=8 and mainly affects the L/W=4 vortex by moving it close to the windward building. These findings suggest that, although spanwise confinement affects the position of the recirculation vortex, the choice of L/W=8 alone cannot be held responsible for the discrepancies observed, as it adequately reproduces the canyon flow structure reported in the literature. It should be noted, however, that the periodic boundary conditions employed with LES effectively represent an infinitely repeating canyon and cannot correspond to the fourth canyon examined in the experiments.

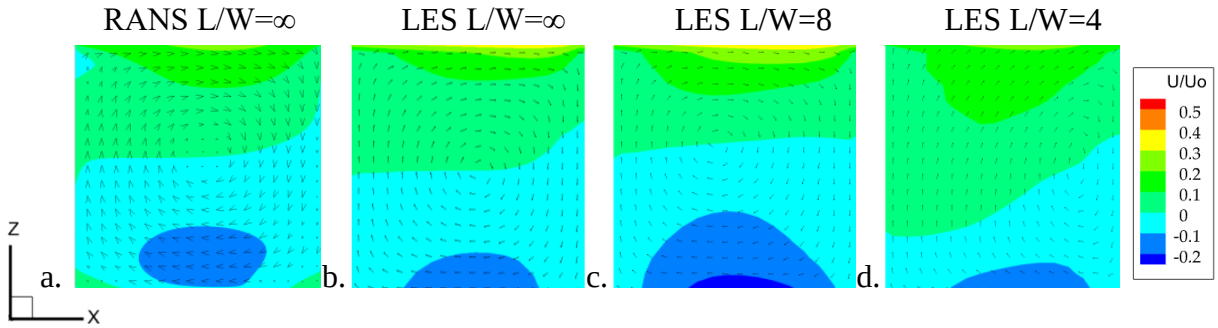

Figure 6 Streamwise velocity and velocity vectors at the mid-canyon plane for the single canyon case

With the single canyon results showing the recirculation vortex also measured in the NTUA experiments, attention focuses on the upwind velocity profiles, which were those measured in NTUA for RANS and corresponded to an infinite upstream fetch for LES. Figure 7 presents isosurfaces of the streamwise velocity, velocity vectors, and the mid-plane distribution of the streamwise velocity for the domain with an inlet at the upstream edge of the roof of the first building in the array. Velocity measurements were applied at this inlet. A well defined recirculation vortex is formed within the canyon, which is consistent across all canyons and closely resembles the structure observed in the idealized infinite canyon cases (Figure 6a,b). It should be noted that in the measured velocity profiles on the roof of the first building in the array, the rooftop recirculation that was observed in the simulations with uniform flow and the splitter plate is not present. This is significant, as the rooftop vortices observed in the full wind tunnel simulations were found to deflect the flow upward, inhibiting its penetration into the canyon and preventing the formation of a coherent in-canyon vortex at the mid-plane (Figure 5). In contrast, the NTUA measurements of velocity profiles on the roofs of the 3rd-5th building

indicate that no rooftop recirculation is present above the downstream buildings. From a physical standpoint, there is a strong indication that the stagnation region and the separation from the leading edge of the first building is a determining factor in how the flow develops over the roofs of the downstream buildings and how it affects the in-canyon flow.

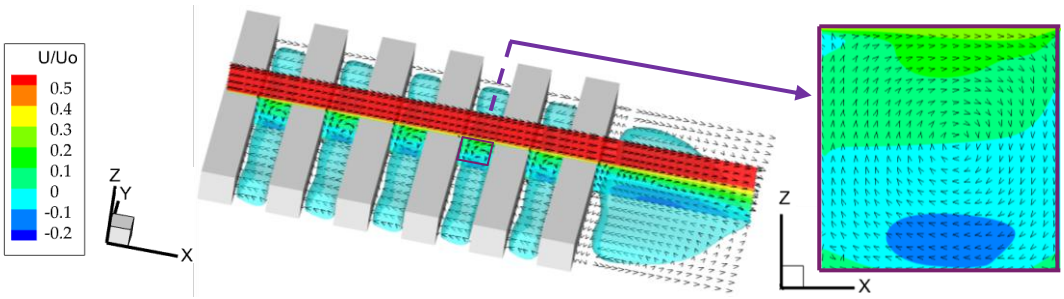

Figure 7 Velocity vectors at the vertical mid-plane and horizontal H/3 plane and streamwise velocity isosurfaces for the roof-level inflow domain

In Figure 8, four different inlet velocity profiles are examined, applied at the upstream domain. Near uniform profiles with varying roughness length (up to H/3) were applied to approximate the incoming flow as it develops downstream of the splitter plate's leading edge. In addition to these cases, a uniform profile was also tested, but it produced identical results to those presented in Figure 5 and is therefore omitted here for brevity. For the smallest roughness length considered ($z_0 = 10^{-4}$ m), the roof vortex is reduced compared to the uniform case (Figure 5), covering only the first two buildings, while two secondary, smaller vortex appear above the third and fourth buildings. No vortex formation is observed within the canyon. As the roughness length increases ($z_0 = 10^{-3}$ m), the recirculation above the fourth roof disappears, while the vortex above the third roof weakens but still no in-canyon vortex is formed. For a further increase in the roughness length ($z_0 = 5 \cdot 10^{-3}$ m), the roof-level recirculation region decreases, while a vortex forms inside the canyon. For a higher value of z_0 ($z_0 = 8 \cdot 10^{-3}$ m), the in-canyon vortex further intensifies and expands. At this stage, the flow qualitatively approaches the NTUA observations (Figure 1), with a similar vortex position, although its size remains significantly smaller in the CFD results.

Figure 9a,b present the streamwise velocity profiles along the canyon centerline for the TWEET-IE data, the Lin et al. (2021) measurements and full set up domain CFD results. In Figure 9a these are compared with the single canyon configurations (RANS and LES (L/W=∞,8,4) and Figure 9b focuses on the influence of inflow configurations, including the roof-level inflow and upstream domain configurations (only the case with $z_0 = 8 \cdot 10^{-3}$ m is shown for the upstream domain). The full-set up domain profile aligns more closely with the TU DELFT data, with qualitatively similar profiles, but quantitative deviations are observed. The LES L/W=∞,8 simulations and the roof-level inflow domain agree well with Lin et al. (2021), within and above the canyon. This is reasonable as Lin et al (2021) had 25 buildings in their array and the LES periodic conditions resemble this situation. The RANS L/W=∞ solution also reproduces Lin et al. (2021) profile within the canyon. The centerline profile of the upstream domain is in agreement with that of the full set-up domain and seems qualitatively similar to that at the TU Delft centerline, even though an in-canyon vortex is formed (Figure 8). Overall, the results indicate that the inlet configuration and domain setup strongly influence the flow structure and vortex position and achieving simultaneous agreement in both flow topology and velocity magnitude remains challenging.

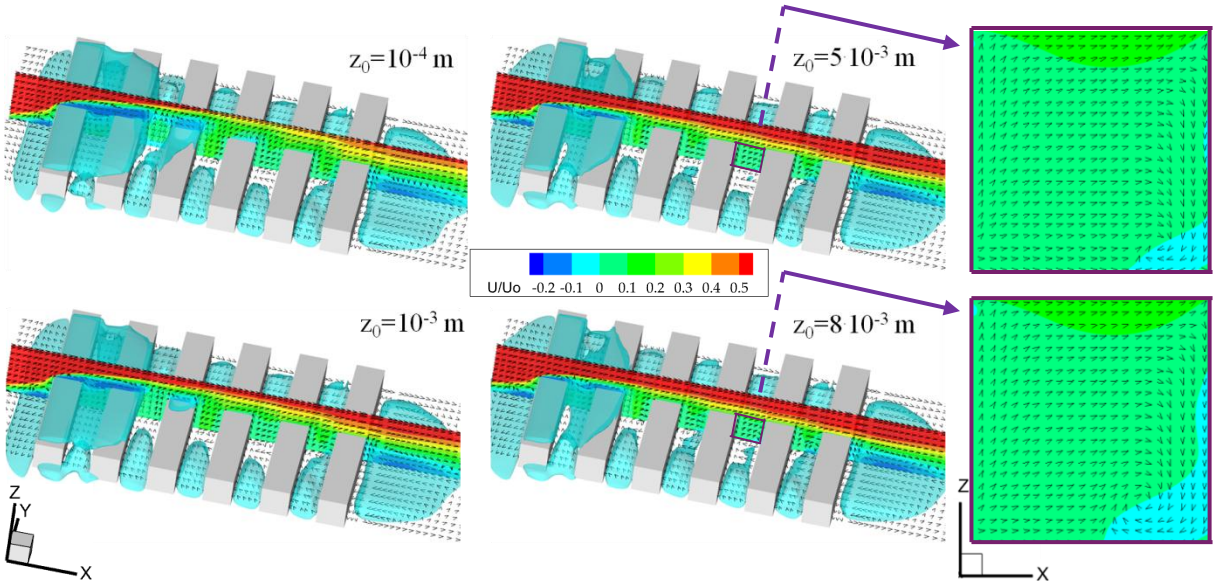

Figure 8 Velocity vectors at the mid-plane and streamwise velocity isosurfaces for the upstream domain

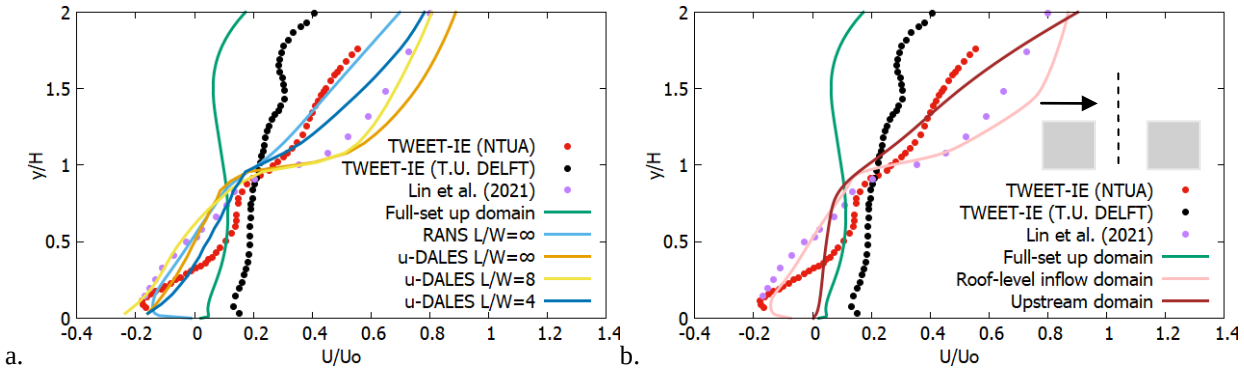

Figure 9 Comparison of Centerline Velocity Profiles TWEET-IE and literature measurements and CFD results of (a) the Full-set up and single canyon domains and (b) Full-set up, Roof-level inflow and Upstream domains.

4. CONCLUSIONS

This study is motivated by the discrepancies observed between twin experiments of the flow in a H/W = 1 street canyon in the NTUA and TU Delft wind tunnels. It examines the sensitivity of the flow to several configuration factors using LES and RANS simulations, focusing on the influence of canyon spanwise length and, particularly, the flow above and upstream of the canyon. CFD simulations of the full setup reproduce a large rooftop recirculation zone covering the first four upstream buildings and canyons. The negative velocities on the roof of the 4th canyon's upstream building in the TU Delft measurements may be an indication of this recirculation zone. In both the full setup simulations and the TU Delft measurements, no in-canyon vortex is observed at the mid-plane of the fourth canyon. Subsequently, RANS simulation was performed for an infinite single canyon using measured rooftop inflow profiles to isolate the effect of inflow conditions, showing that a well-defined in-canyon vortex is consistently reproduced. To investigate whether these discrepancies could be attributed to spanwise effects or unsteady phenomena, LES simulations were performed for infinite and finite-span canyons. The periodic boundaries employed in LES effectively represent infinitely repeating canyons, in which an in-canyon vortex is consistently observed, regardless of spanwise length. These findings indicate that spanwise extent alone does not explain the absence of a

vortex and that the number of upstream canyons plays a key role. Similarly, when the inlet boundary is prescribed at roof level, the flow exhibits behavior consistent with the literature and the infinite canyon, even though the spanwise length remains unchanged. The upstream domain simulations reveal the strong sensitivity to inlet conditions as, variations in the inflow profile, particularly near the ground, significantly affect the canyon flow by modifying the recirculation above the upstream rooftops, leading to flow structure that qualitatively approach the NTUA observations. Overall, the canyon flow is highly sensitive to upstream conditions, the spanwise length influences the vortex position but it doesn't suppress its formation. CFD validation without the upstream flow information may be significantly disadvantaged and sensitivity analysis is recommended to avoid unwarranted pursuit of model related uncertainties.

REFERENCES

Allegrini, J., Dorer, V., Carmeliet, J., 2013.Wind tunnel measurements of buoyant flows in street canyons, Build. Environ. 59 315–326.

American Society of Civil Engineers.,2012. Wind Tunnel Testing for Buildings and Other Structures.

Chew,, L., W., Norford,, L., K., 2018. Pedestrian-level wind speed enhancement in urban street canyons with void decks. Building and Environment, 146, 64–76.

Cui, P.Y., Li, Z., Tao, W.Q., 2014. Investigation of Re-independence of turbulent flow and pollutant dispersion in urban street canyon using numerical wind tunnel (NWT) models, Int. J. Heat Mass Tran. 79 176–188.

Dsouza, B., Pallas, N.P., Yu, W., Bouris, D., Gromke, C. and Sciacchitano, A., 2025. Three-dimensional flow topology and Reynolds number independence in an urban street canyon. 21th International Symposium on Flow Visualization, June 21-25, Tokyo, Japan.

Hunter, L.J., Watson, I.D., Johnson, G.T., 1990. Modelling air flow regimes in urban canyons, Energy Build 15 (3) 315–324.

Kovar-Panskus, A. P., Louka, J.F., Sini, E., Savory, M., Czech, A., Abdelqari, P., Mestayer, N., Toy, 2002. Influence of geometryon the mean flow within urban street canyons—A comparison of wind tunnel experiments and numerical simulations.Water Air Soil Pollut. Focus, 2, 365–380.

Kotsiopoulou, M., Bouris, D., 2022. Numerical Simulation of the Effect of a Single Gust on the Flow Past a Square Cylinder, Fluids 7.9.

Li, Z., Zhang, H., Wen, C.-Y., Yang, A.-S., Juan, Y.-H., 2021. The effects of lateral entrainment on pollutant dispersion inside a street canyon and the corresponding optimal urban design strategies. Building and Environment 195, 107740.

Lin, Y.Y., Hang, J., Yang, H.Y., Chen, L., Chen, G.W., Ling, H., Sandberg, M., Claesson, L., Lam, C.K.C., 2021. Investigation of the Reynolds number independence of cavity flow in 2D street canyons by wind tunnel experiments and numerical simulations, Build. Environ. 201, 107965.

Pallas, N.P, Dsouza, B, Bouris, D., Sciacchitano, A., Gromke, C., 2025. Twin wind tunnel investigation of the scale effects on a street canyon flow. 9th European-African Conference on Wind Engineering (EACWE2025), 16–19 June, Trondheim, Norway.

Suter, I., Grylls, T., Sützl, B. S., Owens, S. O., Wilson, C. E., & van Reeuwijk, M., 2022. uDALES 1.0: a large-eddy simulation model for urban environments. Geoscientific Model Development, 15, 5309–5335.

Tominaga, Y., Mochida, A., Yoshie, R., Kataoka, H., Nozu, T., Yoshikawa, M., Shirasawa, T., 2008. AIJ guidelines for practical applications of CFD to pedestrian wind environment around buildings, J. Wind Eng. Ind. Aerod. 96 1749–1761.

TWEET-IE (2021). Twin Wind Tunnels for Energy and the EnvironmenT – Innovations and Excellence. HORIZON-WIDERA-2021-ACCESS-03, European Commission. Available at: www.tweet-ie.eu.

VDI 3783 part 12, 2000. environmental meteorology: Physical modelling of flow and dispersion processes in the atmospheric boundary layer. applications of wind tunnels.Beuth Verlag.

Vreman, A.W., 2004. An eddy-viscosity subgrid-scale model for turbulent shear flow: algebraic theory and applications. Phys. Fluids 16, 3670–3681.

Uehara, K., Murakami, S., Oikawa, S. Wakamatsu, S., 2000. Wind tunnel experiments on how thermal stratification affects flow in and above urban street canyons, Atmos. Environ. 34 1553–1562.

Zhu, S., Chew, L.W., 2025. Flows across 3D Urban Street Canyons: Revisiting Reynolds Number Independence by Large Eddy Simulation, Build. Environ.113635.